



# The effect of system pressure on microstrain and photoluminescence properties of TiO<sub>2</sub> nanowires

Scientific research paper

Saeideh Ramezani Sani<sup>1\*</sup>, Abdollah Morteza Ali<sup>2</sup>

<sup>1</sup>*Department of Physics, Roudehen Branch, Islamic Azad University, Roudehen, Iran*

<sup>2</sup>*Department of Physics, Alzahra University, Tehran, Iran*

## ARTICLE INFO

### Article history:

Received 16 December 2023

Revised 3 February 2024

Accepted 19 February 2024

Available online 21 March 2024

### Keywords

TiO<sub>2</sub> nanowires

Pressure

Micro strain

Oxygen vacancies

Photoluminescence

## ABSTRACT

TiO<sub>2</sub> nanowires were prepared by a thermal evaporation method at different pressures. The effects of air pressure on morphology, microstructure, and photoluminescence properties were investigated by SEM, XRD, and spectrophotometer. XRD Analysis indicated the presence of rutile phases in samples. The Williamson-Hall method was used for studying micro strain and crystallite size. The results showed that decreasing air pressure leads to increasing micro strain due to increasing tension in the grain boundary with increasing oxygen vacancies as point defects. TiO<sub>2</sub> nanowires prepared at lower pressure indicated weaker intensities in the PL spectrum due to increasing nonradiative centers obtained by oxygen vacancies that as an extinguisher the luminescence may trap photogenerated electron-hole.

## 1 Introduction

The difference in structure of nanomaterial and quantum size effects is due to changing the synthesis conditions that imply new physical and chemical properties. Micro strain is one of the important factors in identifying the physical properties of nanostructures [1]. Micro strain expands the XRD lines. The additional volume of grain boundaries and dislocations are the basic source of micro strain [2]. The production of optical and electrical devices with high quality and lifetime requires films with perfect structure. Strains and stresses on thin films deposited on substrate change the mechanical properties, electronic structure, chemical stability, etc. [3]. Thus, the information about micro strains can improve structural properties.

A broad field of research has been carried out on the correlation between Photoluminescence and mechanical parameters. The results of researches show dependence of PL emission on parameters such as: micro

strain, defects, oxygen pressure, and the crystallite size. Nevertheless; studies in this area are in progress [4-5].

Semiconducting in one-dimension has attracted attention due to unique physical properties. Among them, the TiO<sub>2</sub> with a wide band gap (3.2 eV for anatase and 3.0 eV for rutile) is a suitable candidate due to chemical stability, non-toxic, and low construction cost [6,7], gas sensors [8], optical devices [9,10], photocatalysis [11-13], and solar cells [14]. Different methods such as sol-gel, chemical vapor deposition, hydrothermal, and thermal evaporation have been employed to prepare TiO<sub>2</sub> nanostructure [15–21].

TiO<sub>2</sub> nanostructures deposited on different substrates create different stress effects. In the study of Shibata, the effect of stress on Tio<sub>2</sub> thin films with different substrates such as mica and glass were investigated [22]. In 2015 Rahmani et al. [23] studied the strain phenomena in Tio<sub>2</sub> nanostructures on porous silicon substrates. In 2022 kumavat et al. investigated the micro strain and photoluminescence intensity on Eu

\*Corresponding author.

Email address: S\_ramezanisani@Yahoo.com

DOI: 10.22051/jitl.2024.45857.1105

doped ZnO thin films and observed that the PL intensity and micro strain reduce with Eu doping [24]. Also, in 2013 Dariani and Nafari [25] studied the microstructure properties of the prepared TiO<sub>2</sub> nanowires by thermal evaporation under Ar different flows. But they reported no correlation between PL emission and micro strain. In our previous work in 2020 the microstructure properties of TiO<sub>2</sub> nanowires on Ti substrate were studied by the hydrothermal method [26]. Due to the importance of the dependence of PL emission and micro strain, in this project, we have studied the effects of various air pressures on the micro strain and photoluminescence properties of TiO<sub>2</sub> nanowires. The TiO<sub>2</sub> nanowires were produced in two steps by a thermal evaporation method. The effects of various air pressures on the microstructural and photoluminescence properties were studied.

## 2 Experiment

### 2.1 Fabrication TiO<sub>2</sub> nanowires

By the thermal evaporation method, TiO<sub>2</sub> nanowires were prepared on a silicon substrate. At first, using the evaporation technique, a Ti layer (50 nm) was deposited on the substrate. The pressure and evaporation rates were 10<sup>-5</sup> mbar and 1.5 Å/s, respectively. Then by a sputtering method, an Au thin film with a thickness of 3 nm was deposited as a catalyst on the Ti layer. After this step, in a quartz boat, a mixture of Ti and graphite powder (ratio of 1:1) was placed. The boat was located at the center of a horizontal tube furnace with a temperature of 1050 °C, and the Si substrate was placed in the low-temperature zone (800–850 °C). The sample at 1050 °C temperature was held for 1 h in the 1000 mbar pressure. Then, the sample was cooled down to reach room temperature. In another experiment without changing the parameters of experiment; the air pressure inside the furnace reached to 60 mbar and 30 mbar by a vacuum pump.

### 2.2 Characterization

The morphology and structure of the samples were characterized by scanning electron microscopy, with a voltage of 17 KV and a working distance of 15 mm (SEM: XL130, Philips) and X-ray diffraction (XRD: JEOL JDX- 8030), respectively. The room temperature photoluminescence (PL) spectra of the samples were measured with a Cary Eclipse spectrophotometer.

## 3 Results

### 3.1 morphology properties

Figure 1 indicates the SEM images of TiO<sub>2</sub> nanowires at air different pressures. Figure 1a shows the nanowires with a diameter of around 60 to 120 nm. With decreasing air pressure to 60 mbar, the diameter of the nanowires became smaller (60 to 100 nm) (Fig. 1b), and at pressure equal to 30 mbar, the diameter of nanowires reached 40 to 100 nm (Fig. 1c). For explaining the effect of various air pressures on morphology, the growth mechanism of the prepared TiO<sub>2</sub> nanowires by the thermal evaporation method was considered. Since Au was used as a catalyst, therefore TiO<sub>2</sub> nanowires are grown by the vapor-liquid-solid (VLS) mechanism. According to the VLS mechanism at evaluated temperature, the Ti middle layer is oxidized to TiO<sub>2</sub> by air oxygen. Ti vapour (included source Ti and middle layer Ti) was diffused into the Au catalyst and then a liquid alloy is formed as a nucleation site to grow TiO<sub>2</sub> nanowires. Figure 2 shows the growth process of TiO<sub>2</sub> nanowires schematically. Oxygen plays a basic role in the growth of TiO<sub>2</sub> nanowires. According to the SEM images with reducing air pressure and oxygen, nanowires became thinner. In higher air pressures, increasing oxygen, reaction of the vapor of Ti and O<sub>2</sub> before being absorbed on alloy droplet takes place. Therefore, an increase of oxygen causes a reduction in the growth of TiO<sub>2</sub> nanowires. Also, at lower pressures, the mean free path of particles increases thus, the transfer of gas to the deposition surface is easier.

**Table 1.** The constants of lattice and FWHM of TiO<sub>2</sub> nanowires at different pressures.

pressure(mbar)	unit cell constants		FWHM (degree)
	a(Å)	c(Å)	
1000	4.589	2.961	0.16
60	4.595	2.961	0.19
30	4.599	2.961	0.21

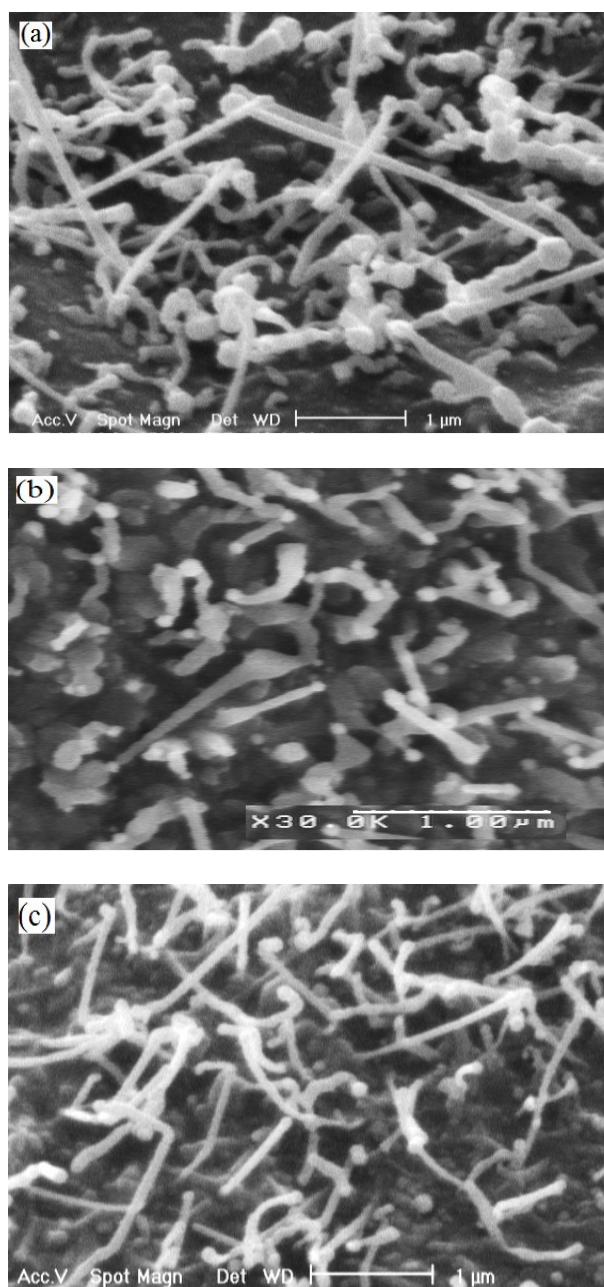


**Figure 1.** SEM images of TiO<sub>2</sub> nanowires (a) 1000 mbar pressure, (b) 60 mbar pressure, (c) 30 mbar pressure. The Scale bar is 1 μm.

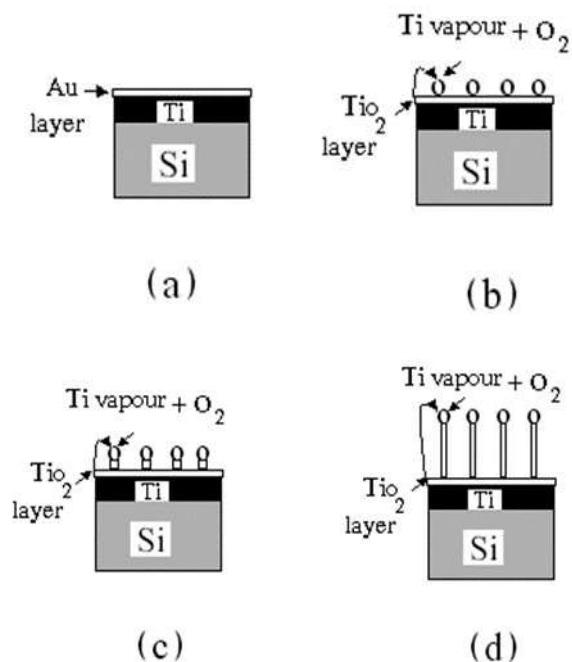


**Figure 2.** The schematic illustration of the growth process of TiO<sub>2</sub> nanowires.

## 3.2 microstructure properties

### 3.2.1 XRD patterns

Figure 3 shows the XRD patterns of TiO<sub>2</sub> nanowires deposited on Si substrate at various air pressures. All the samples show a rutile phase with predominant reflection (101). The constants of the lattice of each sample and the fullwidth at half-maximum (FWMH) were calculated and shown in Table 1, which are in agreement with the value database of (JCPDS #73-1765). Our results showed that with decreasing pressure, the FWHM of (101) peak increases. Also, the intensity of the peak becomes lower. Commonly, in the crystalline with high quality, the FWHM is smaller. With the enhancement of oxygen and reduction of the defects such as oxygen vacancies and titanium interstitials, stoichiometric structures appear. Increasing the pressure from 30 mbar to 1000 mbar creates a high oxygen environment therefore more crystallinity is obtained.

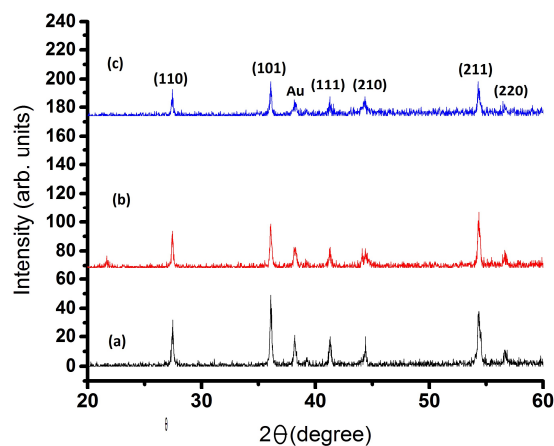


**Figure 3.** XRD patterns of TiO<sub>2</sub> nanowires (a) 1000 mbar pressure, (b) 60 mbar pressure, (c) 30 mbar pressure.

The crystallite size of the nanowires was obtained by the Scherrer equation [27]: ( $D = k\lambda / (\beta \cos \theta)$ ). Where  $K$  is the shape factor,  $\lambda$  is the X-ray wavelength,  $\theta$  is the Bragg angle and  $D$  is the crystallite size. The obtained results are shown in Table 2. It was found with decreasing air pressure the crystallite size decreases.

### 3.2.2 The Williamson -Hall method and micro strain

In the W-H method, the effect of crystal size and micro strains is considered in line with the broadening of XRD. Micro strains correspond to atom displacements to their position in crystals [27]. With separating micro strain and the crystalline size contributions, the sum line breadth is  $\beta = \beta_D + \beta_t$ . Where,  $\beta_D$  is the breadth related to the crystalline size and  $\beta_t$  is the breadth related to micro strain. Therefore the W-H equation is obtained as [28]:

$$\beta = \beta_D + \beta_t = \frac{\lambda}{\beta \cos \theta} + 4\epsilon \sin \theta. \quad (1)$$

Micro strain can be measured from the slope of the curve  $\beta \cos \theta$  vs.  $4 \sin \theta$  and the crystallite size can be calculated from the value of the vertical axis that is cut off by linear fit.

Figure 4 shows the W-H curve of TiO<sub>2</sub> nanowires at various air pressures. It can be seen a positive strain for TiO<sub>2</sub> nanowires at various air pressures which indicates the tensile stress in lattice.

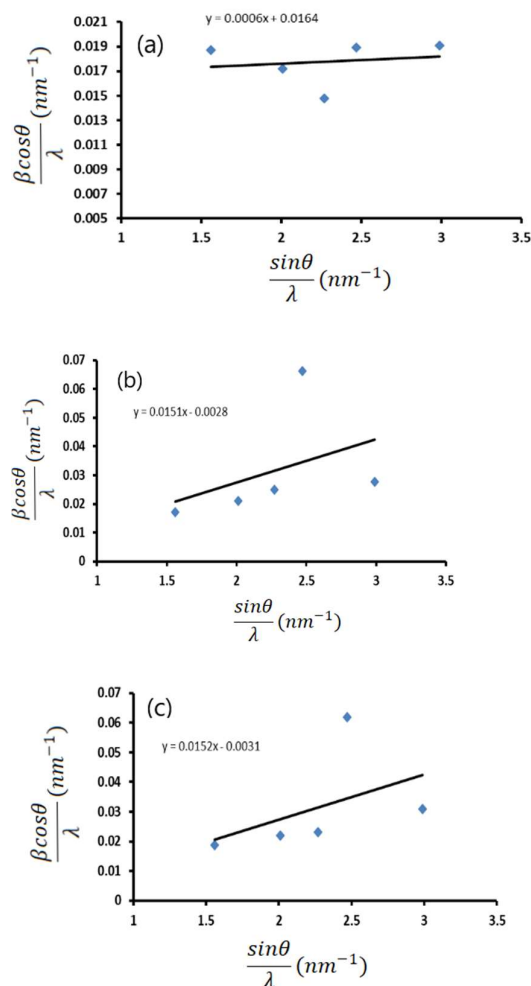


**Figure 4.** Williamson -Hall curve of TiO<sub>2</sub> nanowires (a) 1000 mbar pressure, (b) 60 mbar pressure, (c) 30 mbar pressure.

The obtained value for crystallite size and micro strain of TiO<sub>2</sub> nanowires are shown in Table 2. According to Table 2, A decreasing air pressure leads to an increasing micro strain. The micro strain is proportional to the concentration of defects [2]. With decreasing pressure, oxygen vacancies as point defects can be increased. Thus, increasing the content of oxygen vacancies leads to an increasing tension in the grain boundary and micro strain. Another hypothesis that may confirm increasing micro strain with decreasing air pressure is the enhancement of elastic energy. All of the evaporated particles have a certain kinetic energy. A decreasing air pressure causes reduced collision between evaporated particles, therefore it can increase their velocity and energies and also micro strain.

**Table 2.** Micro strain and crystallite size of TiO<sub>2</sub> nanowires by the Scherrer equation and W-H methods.

pressure(mbar)	W-H methods		Size using Scherrer equation(nm)
	Size(nm)	Micro strain	
1000	60.97	0.0006	56.60
60	35.71	0.0151	47.53
30	32.25	0.0152	44.29

### 3.2.3 Volume strain

Change of volume due to strain is [29]:

$$\theta = \frac{\Delta V}{V} = 2\varepsilon_a + \varepsilon_c, \quad (2)$$

where  $\varepsilon_a$  and  $\varepsilon_c$  are the horizontal and vertical strains, respectively.  $\varepsilon_a$  and  $\varepsilon_c$  can be calculated from [24]:

$$\varepsilon_a = (a - a_0)/a_0 \text{ and } \varepsilon_c = (c - c_0)/c_0, \quad (3)$$

where  $a$  and  $c$  are the strained lattice constant of TiO<sub>2</sub> nanowires while  $a_0=4.587 \text{ \AA}$  and  $c_0=2.954 \text{ \AA}$  are reference values for TiO<sub>2</sub>. Table 3 shows horizontal and vertical strain and volume strain for TiO<sub>2</sub> nanowires at different pressures. It can be seen that the volume strain is positive for all of the samples which indicates the TiO<sub>2</sub> nanowires have been exposed to tensile strain due to tension in the grain boundary with increasing oxygen vacancies as point defects. Comparing the micro strain obtained from the W-H curve and the volume strain calculated from the lattice constant showed that the micro strain and volume strain are same order and positive.

**Table 3.** Horizontal and vertical strain and volume strain for TiO<sub>2</sub> nanowires at different pressures.

pressure(mbar)	$\varepsilon_a$	$\varepsilon_c$	$\theta(\%)$
1000	0.000436 0.00174	0.00236	0.32
60	0.00261	0.00236	0.58
30		0.00236	0.75

### 3.3 Photoluminescence properties

Figure 5. shows the room-temperature photoluminescence of the spectrum of TiO<sub>2</sub> nanowires at various air pressures. The excitation wavelength was 370 nm. According to Fig. 5 there is a strong peak at 435 nm and three weak peaks at 486, 506, and 541 nm. The major peak is due to free exactions emission and weaker peaks can be ascribed to the vacancies of oxygen. [30,31]

Comparing the PL spectra indicated that the relative intensity of all of the peaks has been decreased by changing the pressure from 1000 mbar to 30 mbar. The photoluminescence emission is proportional to both the stoichiometry and the crystallite of the nanostructure [32]. The intensity of emission is estimated using irradiative and non-radiative transmission by  $\eta = I_R / (I_R + I_{NR})$  [33]. Where  $\eta$  is luminescence efficiency,  $I_R$  and  $I_{NR}$  are irradiative and non-radiative transmission, respectively. The crystal imperfections, such as defects, grain boundaries, and dislocations cause the nonradiative transfer. With reducing air pressures and increasing oxygen vacancies, non-radiative centers increase that as an extinguisher the luminescence may trap photogenerated electron-hole [34].

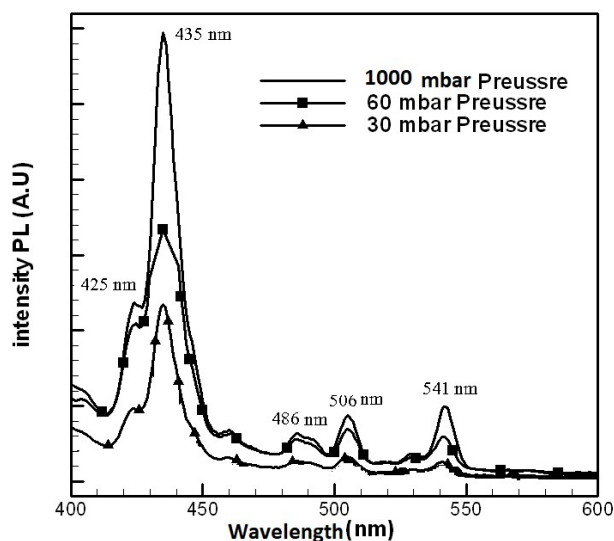


Figure 5. photoluminescence spectrum of TiO<sub>2</sub> nanowires at different system pressures.

## 4 Conclusion

TiO<sub>2</sub> nanowires are fabricated by an evaporation method at different pressures. SEM images showed with decreasing the air pressure, the nanowires become thinner. XRD patterns indicated the rutile phases in the samples. Our results showed that as the air pressure decreases, FWHM of (101) peak increases which leads to weaker crystalline. Also obtained micro strain from the W-H method increases with reducing air pressure. With decreasing pressure, oxygen vacancies as point defects can be increased. Thus, increasing the content of oxygen vacancies leads to an increasing tension in the grain boundary and micro strain due to an increasing tension in the grain boundary. Comparing PL spectra indicated that the relative intensity of all of the peaks has been decreased by changing the pressure from 1000 mbar to 30 mbar. Due to increasing non-radiative centers that as an extinguisher, the luminescence may trap photogenerated electron-hole.

## References

- [1] A. Khorsand Zak, W. H. Abd. Majid, M. E. Abrishami, R. Yousefi, "X-ray analysis of ZnO nanoparticles by Williamson–Hall and size–strain plot methods." *Solid State Sciences*, **13** (2011) 251.
- [2]. I. J. Kingsley; Abdul. Abraham; T. Aderemi; P. Ifeoma; A. Christianah; O. Martins, "Unravelling the effect of crystal dislocation density and microstrain of titanium dioxide nanoparticles on tetracycline removal performance." *Chemical Physics Letters*, **776** (2021) 138725.
- [3] H. Gleskova, S. Wagner, "Electron mobility in amorphous silicon thin-film transistors under compressive strain." *Applied Physics Letters*, **79** (2001) 3347.
- [4] S. Stojadinović, A. Ćirić, "Photoluminescence of ZnO: Eu<sup>3+</sup> and ZnO: Tb<sup>3+</sup> coatings formed by plasma electrolytic oxidation of pure zinc substrate" *Journal of Luminescence*, **235** (2021), 118022.
- [5] I. Choudhary, R. Shukla, A. Sharma, K.K. Raina, "Effect of excitation wavelength and europium doping on the optical properties of nanoscale zinc oxide." *Journal of Materials Science Materials in Electronics*, **31** (2020) 20033.
- [6] Kazuhito Hashimoto, Hiroshi Irie, Akira Fujishima, "TiO<sub>2</sub> photocatalysis: a historical overview and future prospects." *Journal of Applied Physics*, **44** (2005) 8269.
- [7] M. Mehrjouei, S. Müller, D. Möller, "A review on photocatalytic ozonation used for the treatment of water and wastewater." *Chemical Engineering Journal*, **263** (2015) 209.
- [8] A. Rothschild, A. Evakov, Y. Shapira, N. Ashkenasy, Y. Komen, "Surface photovoltage spectroscopy study of reduced and oxidized nanocrystalline TiO<sub>2</sub> films." *Surface Sciences*, **532** (2003) 420.
- [9] E. G. J. Wijnhoven, W. L. Vos, "Preparation of photonic crystals made of air spheres in titania." *Science* **281** (1998) 802.
- [10] A. Richel, N. P. Johnson, D. McComb, "Observation of Bragg reflection in photonic crystals synthesized from air spheres in a titania matrix." *Applied Physics Letters*, **76** (2000) 1816.
- [11] U. Wang, R. T. GUO, Z. X. BI, X. Chen, X.HU, W. Pan. "A review on TiO<sub>2</sub>-x-based materials

- for photocatalytic CO<sub>2</sub> reduction.” *Nanoscale*, **14** (2022) 11512.
- [12] J. Parkash, J. Cho, Y. Kumar Mishra, “Photocatalytic TiO<sub>2</sub> nanomaterials as potential antimicrobial and antiviral agents: Scope against blocking the SARS-COV-2 spread” *Micro and Nano Engineering*, **14** (2022) 100100.
- [13] A. R. Armstrong, J. Ganales, R. Garcia, P. G. Bruce, “Lithium-Ion Intercalation into TiO<sub>2</sub>-B Nanowires.” *Advanced Materials*, **17** (2005) 862.
- [14] U. Bach, D. Lupo, M. P. Comte, J. E. Moser, F. Weissortel, J. Salbeck, H. Spreitzer, M. Gratzel, “Solid-state dye-sensitized mesoporous TiO<sub>2</sub> solar cells with high photon-to-electron conversion efficiencies.” *Nature*, **395** (1998) 583.
- [15] M. Shoostari, J. Salehi, “An electronic nose based on carbon nanotube-titanium dioxide hybrid nanostructures for detection and discrimination of volatile organic compounds” *Sensors and Actuators B: Chemical*, **357** (2022) 131418.
- [16] K. Y. Dong, Y. K. Dong, “Novel approach to the fabrication of macroporous polymers and their use as a template for crystalline titania nanorings.” *Nano Letters*, **3** (2003) 207.
- [17] G. H. Du, Q. Chen, R. C. Che, Z. Y. Yuan, L. M. Peng, “Preparation and structure analysis of titanium oxide nanotubes.” *Applied Physics Letters*, **79** (2001) 3702.
- [18] J. M. Wu, H. Shin, W. T. Wu, Y. K. Tseng, I. C. Chen. “Thermal evaporation growth and the luminescence property of TiO<sub>2</sub> nanowires.” *Journal of Crystal. Growth*, **281** (2005) 384.
- [19] K. Huo, X. Zhng, L. Hu, X. Sun, J. Fu, P. k. Chu, “One-step growth and field emission properties of quasisaligned TiO<sub>2</sub> nanowire/carbon nanocone core-shell nanostructure arrays on Ti substrates” *Applied Physics Letters*, **93** (2008) 013105.
- [20] Y. wang, H. Yang, H. Xu, “DNA-like dye-sensitized solar cells based on TiO<sub>2</sub> nanowire-covered nanotube bilayer film electrodes.” *Materials Letters*, **64** (2010) 164.
- [21] J. T. Mazumder, R. Mayengbam, A. Nath, M. B. Sarkar, “Investigation of structural, optical and electrical properties of TiO<sub>2</sub> thin film-nanowire-based device for photodetector application.” *Optical materials*, **133** (2022) 112936.
- [22] T. Shibata, H. Irie, D. A. Try, K. Hashimoto, “Effect of Residual Stress on the Photochemical Properties of TiO<sub>2</sub> Thin Films.” *The Journal of Physical Chemistry C*, **113** (2009) 12811.
- [23] N. Rahmani, R. Dariani, “Strain-related phenomena in TiO<sub>2</sub> nanostructures spin-coated on porous silicon substrate.” *Superlattices and Microstructures*, **85** (2015) 504.
- [24] A. Kumawat, S. Chattopadhyay, K. Prakash Misra, R. D. K. Misra, P. Kumari, “Micro-strain governed photoluminescence emission intensity of sol-gel spin coated Eu doped ZnO thin films.” *Thin Solid Films*, **761**(2022) 139521.
- [25] R. S. Dariani, Z. Nafari Qaleh, *Thin Solid Films*, “Microstructure characterization of TiO<sub>2</sub> nanowires fabricated by thermal evaporation process.” **542** (2013) 192.
- [26] S. Ramezani Sani, A. Sanei, *Nanomaterials*, “Microstructure Characterization of TiO<sub>2</sub> Nanowires by Hydrothermal Method.” **44** (2020) 223.
- [27] G. Madhu, Vipin C. Bose, K. Maniammal, A. S. Aiswarya Raj, V. Biju, “Microstrain in nanostructured nickel oxide studied using isotropic and anisotropic models.” *Physica B*, **421** (2013) 87.
- [28]. G. K. Williamson, W. H. Hall, “X-ray line broadening from filed aluminium and wolfram.” *Acta Metallurgica*, **1** (1953) 22.
- [29] W. C. Elmore, M. A. Heald, *Physics of Waves*, McGraw-Hill Book Company, USA, 1969.
- [30] K. Keis and A. Roos, “Optical characterization of nanostructured ZnO and TiO<sub>2</sub> films.” *Optical Materials*, **20** (2002) 35

- [31] L. Grabner, S. E. Stokowski, W. S. Brower, “No-Phonon  $^4T_{2g}$ - $4A_{2g}$  Transitions of  $Cr^{3+}$  in  $TiO_2$ .” *Physical Review B*, **2** (1970) 590.
- [32] Z. K. Tang et al., “Room-temperature ultraviolet laser emission from self-assembled ZnO microcrystallite thin films” *Applied Physics Letters*, **72** (1998) 3270.
- [33] S. Shionoya, W. M. Yen (Eds.), *Phosphor Handbook*, Chemical Rubber, Cleveland, 1999.
- [34]. Yan Cong, S. Bin Li, Shumei Yue, and Di Fan, “Effect of Oxygen Vacancy on Phase Transition and Photoluminescence Properties of Nanocrystalline Zirconia Synthesized by the One-Pot Reaction.” *The Journal of Physical Chemistry C*, **113** (2009) 13974